Tree Physiology 34, 619–629
doi:10.1093/treephys/tpu045

Research paper

Leaf-to-branch scaling of C-gain in field-grown almond trees under different soil moisture regimes

Gregorio Egea[1,3], María M. González-Real[2], Bernardo Martin-Gorriz[2] and Alain Baille[2]

[1]Área de Ingeniería Agroforestal, Escuela Técnica Superior de Ingeniería Agronómica, Universidad de Sevilla, Ctra Utrera km 1, 41013 Sevilla, Spain;
[2]Área de Ingeniería Agroforestal, Escuela Técnica Superior de Ingeniería Agronómica, Universidad Politécnica de Cartagena, Paseo Alfonso XIII, 48, 30203 Cartagena, Spain;
[3]Corresponding author (gegea@us.es)

Received March 13, 2014; accepted May 6, 2014; published online June 26, 2014; handling Editor Ülo Niinemets

Branch/tree-level measurements of carbon (C)-acquisition provide an integration of the physical and biological processes driving the C gain of all individual leaves. Most research dealing with the interacting effects of high-irradiance environments and soil-induced water stress on the C-gain of fruit tree species has focused on leaf-level measurements. The C-gain of both sun-exposed leaves and branches of adult almond trees growing in a semi-arid climate was investigated to determine the respective costs of structural and biochemical/physiological protective mechanisms involved in the behaviour at branch scale. Measurements were performed on well-watered (fully irrigated, FI) and drought-stressed (deficit irrigated, DI) trees. Leaf-to-branch scaling for net CO_2 assimilation was quantified by a *global* scaling factor (f_g), defined as the product of two specific scaling factors: (i) a *structural* scaling factor (f_s), determined under well-watered conditions, mainly involving leaf mutual shading; and (ii) a *water stress* scaling factor ($f_{ws,b}$) involving the limitations in C-acquisition due to soil water deficit. The contribution of structural mechanisms to limiting branch net C-gain was high (mean f_s ~0.33) and close to the projected-to-total leaf area ratio of almond branches ($\varepsilon = 0.31$), while the contribution of water stress mechanisms was moderate (mean $f_{ws,b}$ ~0.85), thus supplying an f_g ranging between 0.25 and 0.33 with slightly higher values for FI trees with respect to DI trees. These results suggest that the almond tree (a drought-tolerant species) has acquired mechanisms of defensive strategy (survival) mainly based on a specific branch architectural design. This strategy allows the potential for C-gain to be preserved at *branch* scale under a large range of soil water deficits. In other words, almond tree branches exhibit an architecture that is suboptimal for C-acquisition under well-watered conditions, but remarkably efficient to counteract the impact of DI and drought events.

Keywords: carbon balance, deficit irrigation, photosynthesis, productivity, *Prunus dulcis*, water stress.

Introduction

The almond tree [*Prunus dulcis* (Mill.) D. A. Webb] is a fruit tree species that responds positively to deficit irrigation (DI) programmes, as crop yield may be little affected with significant water reductions (Egea et al. 2010). This excellent response has been ascribed to the fact that some yield-determining processes in many fruit tree species are not sensitive to water stress at some developmental stages (Fereres and Soriano 2007). The mechanisms behind drought tolerance of yield determinants are still unclear, although changes in the partitioning of assimilated carbon (C) are accepted as a plausible explanation (Fereres and Soriano 2007). However, other adaptive processes to water stress that may be acting on net C-assimilation and thus C-balance at the branch/tree level have not been fully explored.

Spatiotemporal variability in C-acquisition among and within tree branches is the result of variations in branch architecture, individual leaf physiological attributes and micro-environmental

factors (i.e., phylloclimate; see Chelle 2005). Plants acclimated to high-irradiance environments have developed branch architectural traits that provide specific mechanisms of light avoidance such as leaf inclination angle and clumping tending (i) to favour irradiance transmission or reflection rather than absorption and (ii) to increase leaf self-shading. As a high-irradiance environment is frequently associated with dry soil conditions, typical of arid or semi-arid regions of the Mediterranean Basin, trees should also cope with the constraint of limited water resources available for the transpiration process. The adaptation of leaf morphological and physiological traits to the interactive impact of both constraints has led to drought-tolerant species, among which the almond tree represents an interesting case study. In drought-tolerant tree species, the architectural design of branches and their spatial distribution within the tree crown are part of a survival strategy to minimize the deleterious impact of (i) supra-optimal irradiance and its corollary processes [high leaf temperature and leaf-to-air vapour pressure deficit (VPD)] and (ii) limited water uptake from roots. The latter increases the diffusional limitations to leaf CO_2 assimilation, thus enhancing processes of photoinhibition. The irradiance environment within the branches is generally strongly heterogeneous, making extremely complex the description and the quantification of branch physiological fluxes—photosynthesis, transpiration and respiration—driven by irradiance availability within the branch along with branch physiological and phylloclimatic variables.

Agronomists and plant physiologists commonly use single-leaf measurements of net CO_2 assimilation to acquire knowledge on how biotic and abiotic stresses (e.g., water stress due to DI management) affect leaf C-gain and subsequent biomass production and crop yield (Synkova et al. 2006, Egea et al. 2011*b*). However, experience has demonstrated the difficulty in extrapolating data collected from single leaves to branch, individual tree or canopy scales because, as mentioned above, the irradiance environment exhibits large spatial and temporal variability, associated with structural and environmental heterogeneity (Palva et al. 2001, Niinemets et al. 2011). Besides leaf clumping, other key factors causing heterogeneity in the irradiance environment within the canopy include gaps in foliage and in canopy crowns due to cultivation practices, spatial variations in leaf orientation angle and seasonal trends in plant phenology and physiology.

Determining to what extent a factor is critical in determining C-gain at higher aggregation levels than the leaf scale has generally been studied by means of more or less complex 3D models of radiative transfer in heterogeneous turbid media. These models provide detailed information on the spatial distribution of irradiance within the studied ecosystem (tree, stand) or subsystem (tree, branch), provided their required inputs (mainly architectural and morphological) are available (e.g., Pearcy and Yang 1996, Sinoquet and Le Roux 2000, Sinoquet et al. 2001). Associated with a leaf photosynthesis model, the radiative model can supply estimates of the C-gain of the studied system. This model-based upscaling approach has helped to substantially increase our understanding of the role played by structural and physiological factors in limiting the C-gain at canopy and single-tree scales (Muraoka and Koizumi 2005, Pearcy et al. 2005).

An alternative to the upscaling approach would be to derive empirical scaling relationships obtained from simultaneous measurements of C-acquisition at the single-leaf level and at the branch/tree level. The advantage of this empirical approach is that it provides results expressed directly in terms of C-gain, without requiring any detailed knowledge of the system architecture or of single-leaf attributes (morphological, biochemical and physiological). Branch/tree-level measurements provide an integration of CO_2 gain or loss of all individual leaves and, as such, they implicitly include the physical (radiative, structural) and biological (development, growth) processes driving the C-gain. Such an approach is based on measurements of branch/tree net CO_2 assimilation requiring specific devices, careful implementation and survey (e.g., Walcroft et al. 2004, Davi et al. 2005, Medhurst et al. 2006), which are not straightforward to implement. An added difficulty is that parallel measurements of dark respiration (wood, fruits and other organs) should also be performed to get a reliable estimate of the total contribution of leaves to the C-gain of the system, and to allow comparison with single-leaf measurements. This might explain why, to our knowledge, there have been up to now no or hardly any attempts to derive such scaling relationships for C-gain in branches.

The present work describes and analyses the C-acquisition pattern at both leaf and branch scales in almond trees growing in a high-irradiance and -temperature environment (southern Spain) and submitted to three contrasted irrigation regimes: a fully irrigated (FI) treatment and two DI treatments. The main objective was to discriminate between the cost (i.e., the negative impact in terms of C-fixation) that purely structural defensive (i.e., stress avoidance) mechanisms driven by high-irradiance and -temperature conditions (i.e., the FI treatment), and structural and physiological defence mechanisms driven by water stress (i.e., DI treatments), play on maximum (sun-exposed) C-assimilation at the branch functional unit. This objective was reached through the identification in situ of leaf-to-branch scaling relationships in field-grown almond trees.

Materials and methods

Experimental site

The study was conducted during a whole growing season in an almond orchard located at the Agricultural Experimental Station of the University of Cartagena (37°35′N, 0°59′W). The 7-year-old almond trees (*P. dulcis* cv Marta, grafted on Mayor rootstock) were planted at a spacing of 7 × 6 m. A schematic representation of the stages of development of almond trees for the same

location can be found in Nortes et al. (2009). The climate at the site is Mediterranean type characterized by warm to hot dry summers and mild winters. The annual values of reference crop evapotranspiration (ET_o) and rainfall for the experimental season were 1133 and 395 mm, respectively. Daily maximum air temperature varied within the range 9.7 °C (winter) to 36.6 °C (summer), whereas the corresponding daily maximum VPD values were 0.1 kPa (winter) and 4.4 kPa (summer). The soil is a deep (>2.0 m) silt-clay-loam soil with a water-holding capacity of ~0.18 m m^{-1} and a mean bulk density of 1.42 g cm^{-3}. Irrigation water is of good quality with a mean electrical conductivity (EC) of 1.1 dS m^{-1} and a low risk of soil salinization. The trees were managed and fertilized following current commercial practices (a routine pesticide program was maintained, pruning was applied manually in December, and no weeds were allowed to grow within the orchard).

Experimental design

Three irrigation treatments were applied to the experimental plots throughout the growing season (mid-March to October) following a randomized block statistical design with three blocks, one replicate per block and 12 trees per replicate. One FI treatment and two drought-stressed (DI) treatments were implemented. In FI, the trees were irrigated to satisfy maximum crop water requirements (ET_c) throughout the growing season. ET_c was calculated using the crop coefficient approach (Allen et al. 1998) and corrected with a coefficient related to the percentage of ground covered by the crop (Fereres and Castel 1981). The two DI treatments were irrigated at ~40 and 25% ET_c (DI_{40} and DI_{25}, respectively) during the whole growing season. A single pipe per tree row with six 4 l h^{-1} pressure compensating drippers per tree (spaced 1 m apart, starting at 0.5 m from the tree trunk) was used. ET_c was estimated as the product of ET_o and a crop coefficient adjusted for tree size following Fereres and Goldhamer (1990). The reference evapotranspiration was calculated from the Penman–Monteith equation (Allen et al. 1998) using the meteorological variables recorded at a nearby weather station. The volumes of irrigation water applied to the treatments were 698, 282 and 183 mm in FI, DI_{40} and DI_{25}, respectively.

Leaf gas exchange measurements

Leaf gas exchange was measured fortnightly in all treatments throughout the growing season (from May to September) with a portable gas exchange system (CIRAS2, PP systems, Hitchin, Hertfordshire, UK). The desired photosynthetic photon flux density (PPFD, μmol m^{-2} s^{-1}) was provided by an internal red/blue LED light source (PC069-1). A CIRAS2 injection system controlled the ambient CO_2 concentration (C_a, μmol CO_2 mol^{-1} air) in the chamber by adjusting the flow of CO_2 from a CO_2 cylinder. The air temperature and actual VPD of chamber air were also recorded by the CIRAS2. Fully expanded and healthy leaves from sun-exposed fruiting branches were selected for gas exchange measurements. Light-saturated leaf net CO_2 assimilation (A_{lm}, μmol m^{-2} s^{-1}) and leaf transpiration (E_{lm}, mmol m^{-2} s^{-1}) were measured on sunny days on at least two leaves per replicate (i.e., at least six leaves per irrigation regime). All leaf gas exchange measurements were performed between 1100 and 1300 h at PPFD ~1500 μmol m^{-2} s^{-1} (saturating PPFD was previously determined in leaves of well-watered almond trees, which was ~1200 μmol m^{-2} s^{-1}) and near-constant C_a (349 ± 4 μmol CO_2 mol^{-1} air).

Branch-level gas exchange measurements

Whole-branch gas exchange was measured with a branch bag open system (PLC-I, PP systems) connected to a portable infrared gas analyser (CIRAS2, PP systems). The PLC-I is a portable open inflatable polyethylene chamber (~25-l capacity) transparent to solar and to infrared irradiance to avoid excessive over-warming. The chamber was attached to the base of each fruit-bearing branch with zip ties and a foam ring to ensure correct sealing. The system measures branch gas exchange from the temporal variations of the differential between incoming and outgoing gas concentrations determined at 1.6-s intervals (dC/dt). An electric fan allows air to flow through the chamber while an additional fan placed inside the bag is used to homogenize the air. Air flow rate, measured by a flow gauge placed in the air inlet, was set to its maximum value (~10 l min^{-1}) to provide a full chamber volume exchange every 2–3 min. Air temperature (T_a) and incident PPFD inside the bag are also monitored by the branch bag system. Whole-branch net CO_2 assimilation (A_{wb}) and transpiration (E_{wb}) rates can be derived from CO_2 and H_2O balance equations (Jones 1992) and measured values of both dC/dt (or dH_2O/dt) and the total leaf area enclosed in the branch bag (L_b). After A_{wb} determination in each sampled branch, the branch was first completely defoliated to measure shoot (R_s) plus fruit (R_f) respiration rate ($R_{sf} = R_s + R_f$) and then completely defruited to determine R_s. Rates of R_{sf} and R_s were subsequently used to derive R_f ($= R_{sf} - R_s$) and branch-level leaf net CO_2 assimilation rate ($A_b = A_{wb} - R_{sf}$). R_s and R_f were measured under similar light regimes and on the same sampling dates as A_{wb}. Season-averaged R_s values, expressed per unit of shoot surface area, were 0.76 ± 0.09 μmol CO_2 m^{-2} s^{-1} (FI), 0.64 ± 0.08 μmol CO_2 m^{-2} s^{-1} (DI_{40}) and 0.63 ± 0.11 μmol CO_2 m^{-2} s^{-1} (DI_{25}). The respective R_f values, expressed per individual fruit, were 0.77 ± 0.40 nmol CO_2 $fruit^{-1}$ s^{-1} (FI), 0.61 ± 0.40 nmol CO_2 $fruit^{-1}$ s^{-1} (DI_{40}) and 0.97 ± 0.30 nmol CO_2 $fruit^{-1}$ s^{-1} (DI_{25}). L_b was measured using an area meter (LI-3100 Leaf Area Meter, Li-Cor, Lincoln, NE, USA), allowing A_b to be expressed in μmol CO_2 m^{-2} leaf s^{-1}. A_b measurements were performed in relatively horizontal (to facilitate chamber handling) sun-exposed branches (hereafter termed A_{bm}) with incident PPFD measured at the top of the branch above saturating values

(PPFD within the range 1467–1955 μmol m^{-2} s^{-1}). Saturating PPFD at branch scale (~1500 μmol m^{-2} s^{-1}) was determined at the beginning of the trial in branches of well-watered almond trees. A_{bm} was determined on three branches (one per replicate) per irrigation treatment on the same sampling dates and times as A_{lm}. Branch bag measurements were performed when the rates of photosynthesis and transpiration were stable, usually within 2–4 min. In the following *branch* net assimilation refers to the net CO_2 assimilation of the *foliar* elements of the branch.

Plant water status measurements

Midday stem water potential (Ψ_t) was monitored with a Scholander-type chamber (Model 3000; Soil Moisture Equipment Corp., Santa Barbara, CA, USA) on the same days as leaf- and branch-CO_2 exchange on at least two leaves per replicate (i.e., at least six leaves per irrigation treatment). For Ψ_t determination, selected leaves near the trunk were wrapped in small black polyethylene bags and covered with silver foil at least 2 h prior to measurement. Micrometric trunk diameter fluctuations were monitored throughout the growing season in six selected trees per treatment (two per replicate), using a set of linear variable displacement transducers (Solartron Metrology, Bognor Regis, UK, Model DF ±2.5 mm, precision ±10 μm) installed on the northern side of trunks, 40 cm above the ground and mounted on holders built of aluminium and invar—an alloy comprising 64% Fe and 35% Ni that has minimal thermal expansion. Measurements were taken every 30 s, and 10-min means were recorded by a CR10X data logger (Campbell Scientific, Inc., Logan, UT, USA). Maximum daily trunk shrinkage (MDS), which has been proven to be a sensitive and reliable water status index in almond trees (Goldhamer and Fereres 2001), was calculated as the difference between the daily maximum and minimum trunk diameters.

Scaling factors

Leaf-to-branch scaling for net CO_2 assimilation (A) was quantified by means of a *global* scaling factor (f_g), defined as the ratio of the light-saturated net foliar assimilation of the branch (A_{bm}) under the prevailing soil moisture conditions to the net leaf assimilation at saturating-light and under unstressed conditions ($A_{lm,FI}$):

$$f_g = \frac{A_{bm}}{A_{lm,FI}} \quad (1)$$

This factor was assumed to be the product of two specific scaling factors: (i) a *structural* scaling factor (f_s) mainly involving mutual shading; and (ii) a *water stress* scaling factor ($f_{ws,b}$) involving the limitations in C-acquisition at the branch level due to soil water deficit:

$$f_g = f_s \cdot f_{ws,b} \quad (2)$$

with

$$f_s = \frac{A_{bm,FI}}{A_{lm,FI}} \quad (3)$$

and

$$f_{ws,b} = \frac{A_{bm,DI}}{A_{bm,FI}} \quad (4)$$

In a similar way, a leaf water stress factor was defined as

$$f_{ws,l} = \frac{A_{lm,DI}}{A_{lm,FI}} \quad (5)$$

As Eq. (3) supplies the structural factor for FI trees, the factor $f_{ws,b}$ for water-stressed trees implicitly integrates the effects on branch assimilation of physiological limitations together with architectural and morphological changes due to water stress. Note also that f_s includes the effects of physiological and/or biochemical limitations not related to soil water deficit (see the Discussion section).

Radiation interception efficiency of almond branches

The impact of almond branch architecture on radiation interception efficiency was approached by estimating the projected-to-total leaf area ratio of six sampled almond branches (Planchais and Sinoquet 1998) of the FI treatment. Three branches were taken from the shaded part of the crown whereas the remaining three branches were taken from the sunny side of the tree crown. The sampled branches were immediately taken to the laboratory in carefully sealed plastic bags containing wet cotton-made discs to minimize leaf dehydration. Once in the laboratory, each hand-held branch was placed on a white background and a picture was taken in the vertical projection. Then, each branch was manually defoliated to determine (i) the projected leaf area of the non-foliar organs (i.e., wood and fruits) by taking a picture in the vertical projection, as described previously, and (ii) the total leaf area by means of a leaf area meter (LI-3100 Leaf Area Meter, Li-Cor). Pictures were taken in the vertical projection to reproduce a (solar) view angle of similar magnitude to that existing in the field when the gas exchange measurements were performed. The projected leaf area of the different branches was determined using the image-processing package ImageJ (Abramoff et al. 2004).

Statistical analyses

Relationships between tree water status indicators with (i) maximum leaf- and branch-scale net CO_2 assimilation rate and (ii) the global reduction factor were analysed by linear regressions. The coefficient of determination (R^2) and the standard

error of the estimate (SEE) were used as a measure of the accuracy of the linear regressions performed. All analyses were accomplished using the statistical software Statgraphics Centurion XV.

Results

Tree water status

Tree water status was markedly affected by the irrigation regimes (Figure 1). Fully irrigated trees maintained Ψ_t and MDS values within the range −0.6 to −1.2 MPa (Figure 1a) and 240 to 650 μm (Figure 1b), respectively, throughout the season. Deficit irrigated trees showed significantly lower Ψ_t values than FI trees, with minimum values (−2.0 and −2.3 MPa in DI_{40} and DI_{25}, respectively) being reached in the period DOY 180–210. Maximum daily trunk shrinkage in DI trees was also significantly higher than in FI trees, reaching 930 and 1020 μm in DI_{40} and DI_{25}, respectively, in the period DOY 180–210.

Leaf- and branch-level gas exchange

Light-saturated leaf and branch net CO_2 assimilation (A_{lm} and A_{bm}, respectively) showed a similar seasonal pattern in the three treatments (Figure 2), with minimum values occurring in the period DOY 180–210, that is, at the kernel-filling stage (Nortes et al. 2009). Soil moisture regimes had a high impact

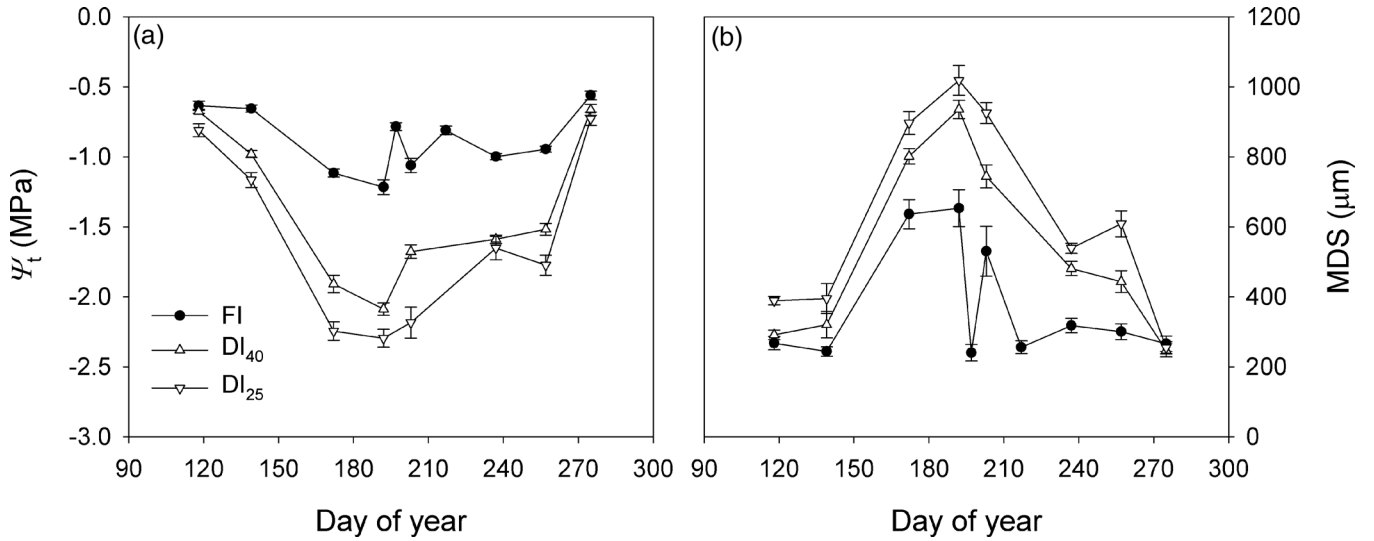

Figure 1. Seasonal time-course of (a) midday stem water potential (Ψ_t) and (b) MDS determined for FI and DI trees (DI_{40} and DI_{25}). Error bars denote ±SE.

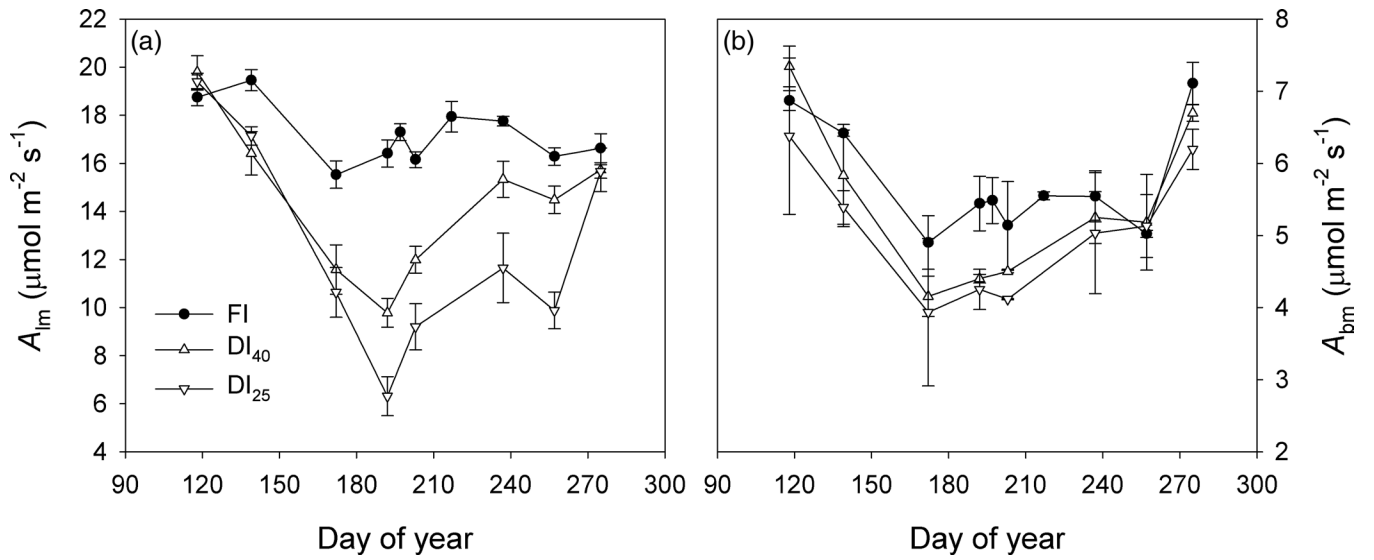

Figure 2. Seasonal time-course of (light-saturated) net CO_2 assimilation rate (a) at leaf scale (A_{lm}) and (b) at branch scale (A_{bm}) determined for FI and DI trees (DI_{40} and DI_{25}). Error bars denote ±SE.

Table 1. Mean seasonal values of maximum transpiration (E), net photosynthesis (A) and instantaneous water-use efficiency (A/E) at both leaf (subscript 'lm') and branch (subscript 'bm') scales.

	A_{lm} (μmol m^{-2} s^{-1})	E_{lm} (mmol m^{-2} s^{-1})	A_{bm} (μmol m^{-2} s^{-1})	E_{bm} (mmol m^{-2} s^{-1})	A_{lm}/E_{lm} (μmol mmol^{-1})	A_{bm}/E_{bm} (μmol mmol^{-1})
FI	17.22a	4.70a	5.77	1.37	3.60	4.36
DI_{40}	14.39ab	4.10a	5.63	1.40	3.57	4.14
DI_{25}	12.74b	3.42b	4.87	1.19	3.74	4.25
P	0.03	0.001	0.11	0.2	0.94	0.89

Mean values followed by different letters within the same columns indicate significant differences according to Duncan's multiple range test.

on A_{lm} (Figure 2a), which exhibited season-averaged rates significantly different among FI and DI treatments (17.22, 14.39 and 12.74 μmol m^{-2} s^{-1} in FI, DI_{40} and DI_{25}, respectively) (Table 1). However, the corresponding impact on season-averaged A_{bm} (Figure 2b) was moderate, with no significant differences among the treatments (5.77, 5.63 and 4.87 μmol m^{-2} s^{-1} in FI, DI_{40} and DI_{25}, respectively) (Table 1). The same water stress response was observed for E_{bm} and E_{lm} (Table 1). Instantaneous water-use efficiency, defined as the A/E ratio, was conservative irrespective of soil water deficit at both scales of study (Table 1). Season-averaged A/E was ~16% higher at branch than at leaf scale.

Scaling factors

The seasonal pattern of the different scaling factors (Figure 3) was derived from the data presented in Figure 2. The structural factor (f_s) was rather conservative over the observation period, varying in the range 0.32–0.40 in the FI treatment (Figure 3a). During the spring–summer period (DOY 110–240), f_s was fairly constant and close to 0.33. The seasonal time-course of the branch-level water stress scaling factor ($f_{ws,b}$) showed a more variable trend throughout the season (Figure 3b), in agreement with the seasonal variation in tree water status observed in DI_{40} and DI_{25} with respect to FI (Figure 1). $f_{ws,b}$ was close to 1 at the onset of the season in the two deficit treatments, reaching the lowest values by DOY 200 (0.80 and 0.78 in DI_{40} and DI_{25}, respectively). The global reduction factor ($f_g = f_s \cdot f_{ws,b}$) varied within a lower range in FI (0.31–0.43) than in the deficit treatments (0.25–0.40 and 0.25–0.37 in DI_{40} and DI_{25}, respectively) (Figure 3c).

Relations with tree water status indicators

The relationship between Ψ_t and (i) branch- and (ii) leaf-water stress scaling factors derived for DI_{40} and DI_{25} (Figure 4) showed that A_{lm} was ~3.4-fold more sensitive to water stress than A_{bm}, as denoted by the slopes of the corresponding regression lines (0.08 and 0.27 MPa^{-1}) for branch- and leaf-level measurements, respectively.

The relationship between f_g and (i) Ψ_t (Figure 5a) and (ii) MDS (Figure 5b) was linear in both cases. Ψ_t explained nearly 70% of the observed variance in f_g across the season and irrigation treatments (Figure 5a), whereas MDS explained only 57% of the f_g variance.

Discussion

Global cost of branch functioning on C-fixation

In terms of global cost on branch C-acquisition (i.e., f_g), the FI and DI treatments presented a similar seasonal trend, with the minimum of f_g occurring by the middle of the kernel-filling stage (DOY 180–210), corresponding to a period of the year with harsh environmental conditions associated with high values of radiative load, air temperature and VPD. Under these conditions, the minimum values of f_g varied from 0.32 for the FI treatment, to 0.25 for the DI treatments (Figure 3c). This indicates that the global cost of branch functioning on C-acquisition was high (68 and 75% of A_{lm}, respectively, for FI and DI), but not substantially different among well-watered and water-stressed trees, at least for the water stress levels reached in this experiment. This finding represents an important step towards the explanation of the excellent productive response of almond trees under DI strategies (Egea et al. 2010). Indeed, in previous experiments it was observed that kernel yield, once normalized for tree size by expressing it per unit of trunk sectional area, did not differ among well-watered and water-stressed almond trees that received ~30% ET_c (Egea et al. 2010), despite A_{lm} being ~40% lower in the DI treatment over the kernel-filling stage (Egea et al. 2011*a*). The almond yield reduction observed in the DI trees was therefore determined mainly by the impact of water stress on tree size (Egea et al. 2010).

Impact of biochemical limitations on f_s

Because most of the leaves experienced mutual shading, it could be expected that biochemical limitations driven by high radiative load (i.e., photoinhibition) were strongly attenuated within the branch of both FI and DI trees, leading to higher light-use efficiency at branch scale than at leaf scale. It has been reported that biochemical limitations to net CO_2 assimilations play an important role in regulating A_l of almond leaves in FI and DI trees (Egea et al. 2011*b*). High radiative load associated with high leaf-to-air temperature difference and leaf-to-air VPD has been observed to down-regulate the photosynthetic capacity of non-deciduous (Jifon and Syvertsen 2003) and deciduous (Matos et al. 1998) trees. Light-saturated A_l at ambient CO_2 occurs at ~1200 μmol m^{-2} s^{-1} in sun-exposed almond leaves (De Herralde et al. 2003) (i.e., at 45% of the maximum incident PPFD in our experimental area).

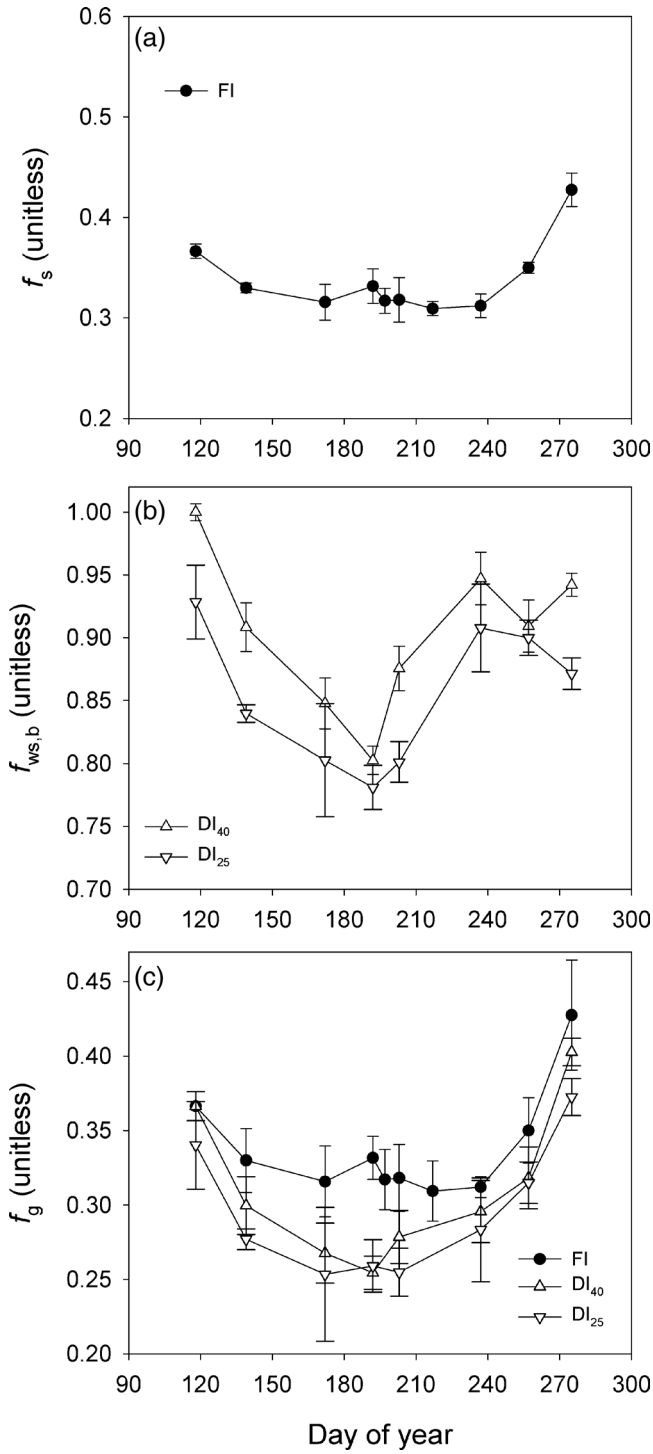

Figure 3. Seasonal time-course of scaling factors: (a) structural (f_s), (b) branch-level water stress ($f_{ws,b}$) and (c) global reduction (f_g) factors determined for FI and DI trees (DI_{40} and DI_{25}) as described by Eqs (1–4). Error bars denote ±SE.

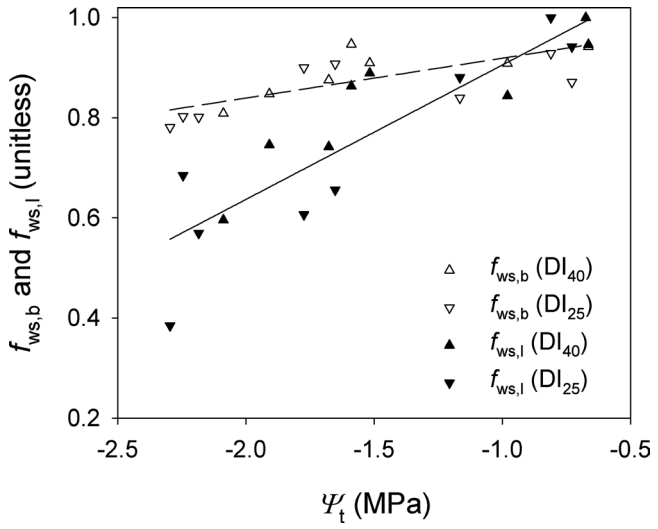

Figure 4. Relationship between stem water potential (Ψ_t) and (i) branch- ($f_{ws,b}$, Eq. 4) and (ii) leaf-water stress factor ($f_{ws,l}$, Eq. 5) for DI trees (DI_{40} and DI_{25}). Regression equations for branch- (open symbols) and leaf-level (filled symbols) measurements (branch: $y = 1.00 + 0.08x$, $R^2 = 0.56$, SEE = 0.04; leaf: $y = 1.17 + 0.27x$, $R^2 = 0.78$, SEE = 0.09). SEE, standard error of the estimate.

Under high values of PPFD, Matos et al. (1998) observed in almond leaves an increase in the minimal fluorescence intensity (F_0) and a large decrease in the ratio of variable to maximum fluorescence (F_v/F_m, the maximum efficiency of photosystem II, PSII) with respect to the values observed at dawn, which are indicative of reversible photoinhibition. The impact of radiation-induced limitations to net CO_2 assimilation was implicitly accounted for in f_s, as far as they may act independently of the occurrence of soil water stress (Valladares et al. 2005), leading to an overestimation of the actual f_s. However, the error was likely to be small because of the reversibility of the radiative stress. Moreover, it is known that the photosynthetic capacity of leaves acclimates to reduced light availability (e.g., Rijkers et al. 2000). In recent work, Egea et al. (2012) showed that leaves located at the south periphery of the almond tree crown (sunlit branches) had significantly higher photosynthetic capacity than leaves of northwest-facing inner shoots that were exposed to substantially lower irradiance. Although the light gradient within a sunlit branch could drive photosynthetic acclimation in shaded leaves and lead to underestimating f_s, this situation is not likely to occur in the same leaves of sunlit branches during a long period because leaf shading depends on beam direction and is transient in a large proportion of leaves. The mean value of f_s (=0.33) indicates that the structural cost on C-acquisition was high, as it represented approximately two-thirds of the C-gain (A_{lm}) of a sun-exposed leaf.

Structural factor, light capture and branch architecture

The structural scaling factor, as defined in this study, could be compared with the parameter ε, defined as the ratio between projected (on a particular direction) and total leaf area (Planchais and Sinoquet 1998, Pearcy et al. 2005). ε is a purely geometrical parameter quantifying the effectiveness of the spatial distribution of leaf area for the interception of

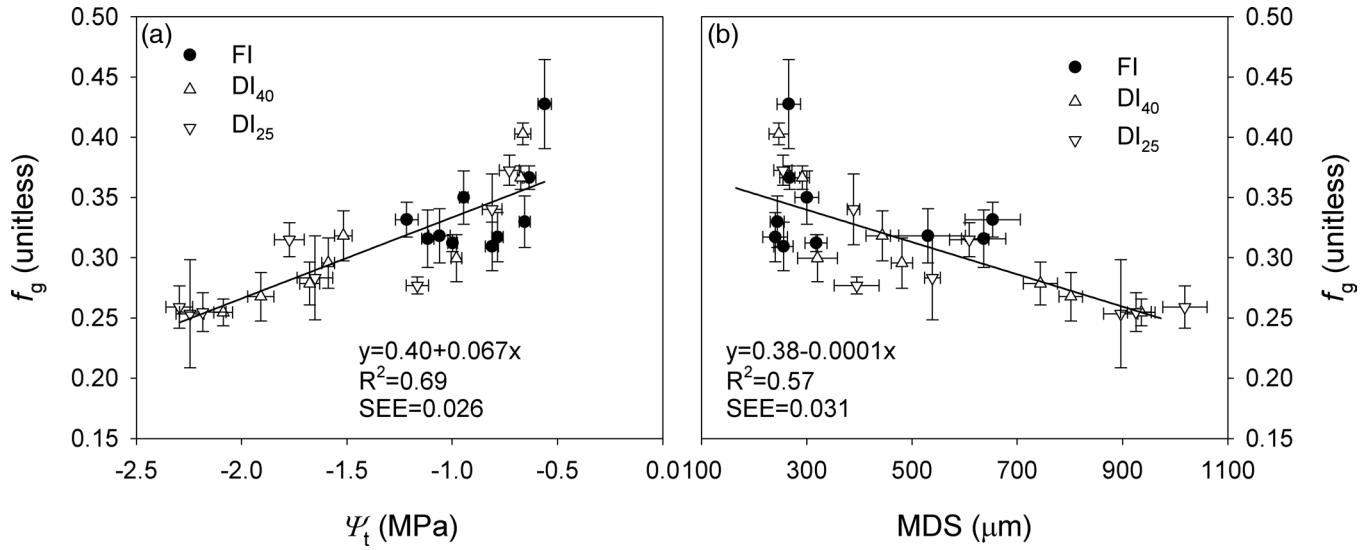

Figure 5. Relationship between global reduction factor (f_g) and (a) stem water potential (Ψ_t) and (b) MDS for pooled data of FI, DI_{40} and DI_{25} trees. Straight lines represent the best-fit regression lines. Error bars denote ±SE.

incident PPFD. As such, ε depends on leaf angle distribution, inclination and azimuth, on the fraction of branch volume occupied by the non-foliar organs (wood, fruits), and on the mutual shading of leaves that may be analysed in terms of space occupation by the branch and leaf dispersion within the space occupied by vegetation (Planchais and Sinoquet 1998).

The low values of f_s reported in this study can probably be ascribed to a low efficiency in PPFD capture by leaves (small ε value). One of the few references found in the literature in which net C-gain was assessed simultaneously at both leaf and branch scales (Le Roux et al. 1999) revealed that f_s of walnut trees (~0.38) is of similar order of magnitude to that of almond trees. As shown in Figure 6, almond leaves present strong leaf clumping due to rosette-like aggregation (Heerema et al. 2008), which causes heavy mutual shading of most of the leaves within the branch volume, decreasing strongly the amount of available PPFD on the leaves, and therefore the leaf assimilation rate. Previous work (e.g., Massonnet et al. 2008) already highlighted that species (or cultivars) with greater leaf clumping and self-shading reduce light interception for a given leaf area. This radiation-avoidance strategy therefore has a cost in terms of reduced C-gain.

The analysis of the architecture of the fruit-bearing shoots in the FI treatment (Figure 7) revealed that ε averaged 0.31 and 0.42 for sunny and shaded branches, respectively. The close agreement between the mean values of ε (=0.31) and f_s (=0.33) for sun-exposed branches (Figure 3a) indicated that their architectural design, such as leaf clumping (rosette-like aggregation), and alternate leaf arrangement along the shoot axis are the main factors responsible for the low values of f_s in FI trees. A corollary conclusion is that radiation-induced stress does not significantly affect the structural factor in well-watered trees. The reduced self-shading found in shaded branches, when compared with sunny ones (Figure 7), is a reported adaptive response allowing plants to increase light capture under reduced light availability (Planchais and Sinoquet 1998).

Figure 6. Almond branch picture showing the spatial distribution of leaves within the space occupied by vegetation (FI treatment).

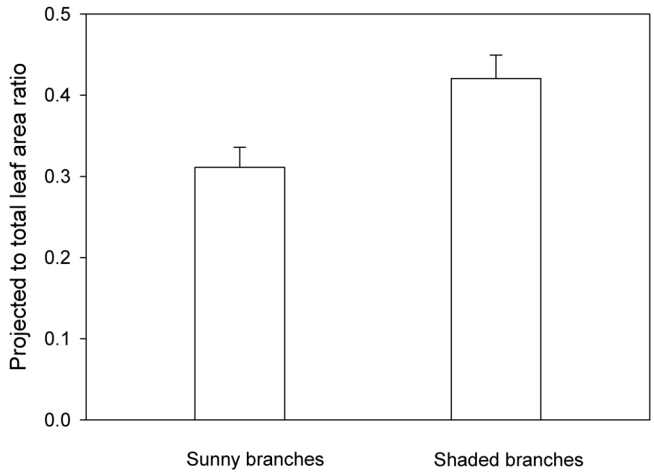

Figure 7. Projected-to-total leaf area ratio (unitless) measured in sunny and shaded almond branches of FI trees. The values are means of three branches ($n = 3$). The error bars denote the standard error of the mean.

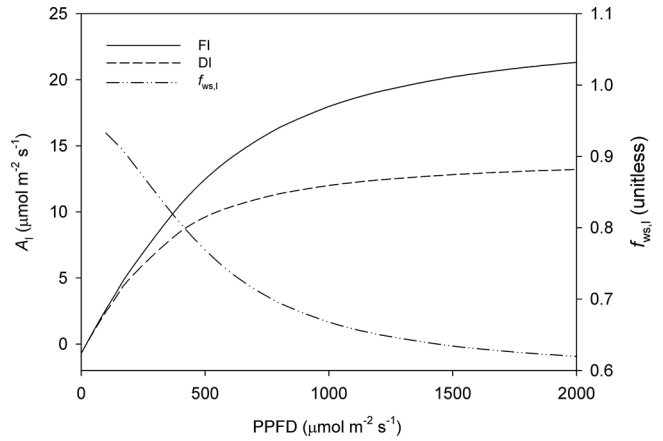

Figure 8. Light-response curve of (i) leaf net photosynthesis rate (A_l) for well-watered (FI) and water-stressed (DI) almond trees, and (ii) leaf-level water stress factor ($f_{ws,l}$). Values are taken from a previous experiment (Egea et al. 2011*b*). Deficit irrigated trees were irrigated at ~40% ET_c over the irrigation season.

Branch vs leaf sensitivity to water stress

Foliar C-acquisition of sunny branches was found to be much less sensitive (by a factor of 3.4) to Ψ_t than that of sun-exposed leaves (Figure 4). A first explanation could be sought in the light-response curves of A_l for FI and DI trees (Figure 8), which indicated that the leaf water stress factor, $f_{ws,l}$, decreased rapidly with increasing PPFD. As shown by Niinemets et al. (2011), the leaf average PPFD at branch scale is significantly lower than the incoming PPFD above the branch, the greater the leaf area index the greater the PPFD gradient. These authors also state that the strong PPFD gradients observed in their analyses may be even greater for aggregated foliage dispersions, such as those of almond trees. Consequently, the leaf average PPFD of almond branches is lower than that received by the outer leaves and thus much lower than that experienced by a sun-exposed leaf, explaining in part the large difference observed in sensitivity to water stress (i.e., Ψ_t) at both scales of study (Figure 4). Secondly, the branch architecture (e.g., leaf mutual shading) is likely to lead, when compared with sun-exposed leaves, to a less stressful within-branch environment (phyllocli-mate), reflected in a higher amount of diffuse radiation, lower surface temperature and surface-to-air VPD, which contributed to the reported lower sensitivity of branches to water stress (Figure 4). A third factor that might be playing a role in the differential response to water stress is the higher sensitivity of A_{lm} to Ψ_t observed in sun-exposed leaves when compared with shaded leaves, from reanalysed data of a previous experiment with almond trees (Egea et al. 2012) (results not shown). Therefore, the high number of shaded leaves within sunny branches could also be contributing to reduce the sensitivity to water stress of C-gain at branch scale with respect to leaf scale. In agronomical terms, this may be a relevant finding on the early detection of water stress for irrigation scheduling, as it would support the use of plant-based indicators determined at leaf scale against other indicators determined at higher scales of study (e.g., branch, tree or stand level). The fact that water-use efficiency remained constant with water stress at both leaf and branch scales (Table 1) points out that C-gain and water lost by transpiration showed a similar sensitivity to soil water deficit at the leaf and branch levels. Similar findings have already been reported for leaf-level measurements performed in field-grown almond trees (Egea et al. 2011*a*), but no reports are available for this species at higher hierarchical levels. A higher (~16%) A/E ratio at branch scale, when compared with leaf-level measurements, was also found in whole-canopy measurements performed in grapevines (Pérez-Pena 2004). An explanation for this branch-level increase in water-use efficiency can be found in lower within-branch surface temperature and surface-to-air VPD (Heilmeier et al. 2002) and/or in curvature differences in the response curve of A and stomatal conductance (g_s) to light, leading to differences in A/g_s with the level of light.

Global impact vs tree water status indicators

Maximum daily trunk shrinkage and Ψ_t are currently used as indicators of tree water status for irrigation scheduling in almond trees (Goldhamer and Fereres 2001). The fact that both water status indicators were highly correlated with f_g (Figure 5), that is, the total cost for branch C-acquisition, represents a promising step towards the development of simple algorithms to predict the effects of multiple environmental drivers on the C balance of the tree at higher hierarchical levels than leaves and, eventually, on crop yield. We found that MDS explained a lower percentage ($R^2 = 0.57$) of the observed variability of f_g across treatments and seasons than Ψ_t ($R^2 = 0.69$), thus indicating that the latter is more suitable to predict the

effects of soil water stress on branch C-acquisition of almond trees. The high number of factors, besides water stress, that act on the magnitude of the diurnal cycles of the tree trunk (Egea et al. 2009) may explain the poorer predictive power of MDS.

Concluding remarks

Over the ages, trees from arid and semi-arid regions have forged a defensive (e.g., stress-avoidance/tolerance) strategy by shaping functional and architectural traits to cope with multiple environmental constraints (e.g., high solar radiation load, low soil moisture, poor shallow soils, etc.). The main conclusion of our study is that almond trees appear to have developed a radiation-avoidance strategy—inherent to its branch structural attributes—that is quite efficient under the abiotic conditions prevailing in their natural habitat (i.e., arid and semi-arid regions with high radiation, temperature and VPD levels and low soil moisture content). The benefit of this avoidance strategy is to make almond trees much less sensitive/responsive to soil water stress at the branch unit, and therefore at the whole-tree scale. This radiation-avoidance strategy implies the following consequences:

(i) Sun-exposed leaves, which act as a radiation shield for the remaining leaves, are subjected to severe abiotic stress, and therefore have to use biochemical/physiological defence mechanisms to survive under such conditions. Such leaves therefore pay a high cost for C-fixation, as indicated by the substantial decrease of their photosynthetic capacity with increasing water stress (see published data on A_{lm} of sun-exposed leaves under the different irrigation treatments, e.g., Nortes et al. 2009). On the other hand, the remaining leaves, more or less shaded, grow in a more suitable environment and maintain a relatively high potential for C-fixation, although receiving less radiation. In other words, sun-exposed leaves bear most of the cost, and the remaining leaves bear most of the benefit derived from the radiation-avoidance strategy. The trade-off is likely to be positive (more benefits than costs) as sun-exposed leaves represent only a small fraction of the branch leaf area.

(ii) The collateral effect of this predominant radiation-avoidance strategy is that branches of FI trees exhibit only slightly better performance in terms of C-gain when compared with water-stressed ones. In other words, almond tree branches exhibit an architecture that is suboptimal for C-acquisition under well-watered conditions, but rather efficient to counteract the impact of irrigation water deprivation and drought.

The tight correlation found between tree water status and f_g, that is, the total cost for branch C-acquisition, provides a simple tool to assess the effects of DI (within the range of water stress reached in this study) on C-assimilation at a higher hierarchical level than leaves in field-grown almond trees.

Conflict of interest

None declared.

Funding

This work was supported by the European Commission (grant number FP7-KBBE-2009-3-245159, SIRRIMED project).

References

Abramoff MD, Magalhaes PJ, Ram SJ (2004) Image processing with ImageJ. Biophotonics Int 11:36–42.

Allen RG, Pereira LS, Raes D, Smith M (1998) Crop evapotranspiration. Guidelines for computing crop water requirements. Irrig. Drain. Paper No. 56. FAO, Rome, Italy, p 300.

Chelle M (2005) Phylloclimate or the climate perceived by individual plant organs: what is it? How to model it? What for? New Phytol 166:781–790.

Davi H, Dufrêne E, Granier A, Le Dantec V, Barbaroux C, François C, Breda N (2005) Modelling carbon and water cycles in a beech forest Part II: validation of the main processes from organ to stand scale. Ecol Model 185:387–405.

De Herralde F, Biel C, Savé R (2003) Leaf photosynthesis in eight almond tree cultivars. Biol Plant 46:557–561.

Egea G, Pagán E, Baille A, Domingo R, Nortes PA, Pérez-Pastor A (2009) Usefulness of establishing trunk diameter based reference lines for irrigation scheduling in almond trees. Irrig Sci 27:431–441.

Egea G, Nortes PA, González-Real MM, Baille A, Domingo A (2010) Agronomic response and water productivity of almond trees under contrasted deficit irrigation regimes. Agric Water Manag 97:171–181.

Egea G, Dodd IC, González-Real MM, Baille A, Domingo R (2011*a*) Partial root zone drying improves almond tree leaf-level water use efficiency and water status during the afternoon compared to deficit irrigated plants at similar soil water status. Funct Plant Biol 38:372–385.

Egea G, González-Real MM, Baille A, Nortes PA, Díaz-Espejo A (2011*b*) Disentangling the contributions of ontogeny and water stress to photosynthetic limitations in almond trees. Plant Cell Environ 34:962–979.

Egea G, González-Real MM, Baille A, Nortes PA, Conesa MR, Ruiz-Salleres I (2012) Effects of water stress on irradiance acclimation of leaf traits in almond trees. Tree Physiol 32:450–463.

Fereres E, Castel JR (1981) Drip irrigation management, Leaflet 21259. Division of Agricultural Sciences, University of California.

Fereres E, Goldhamer DA (1990) Deciduous fruit and nut trees. In: Stewart BA, Nielsen DR (eds) Irrigation of agricultural crops. American Society of Agronomy, Madison, pp 987–1017.

Fereres E, Soriano MA (2007) Deficit irrigation for reducing agricultural water use. J Exp Bot 58:147–159.

Goldhamer DA, Fereres E (2001) Irrigation scheduling protocols using continuously recorded trunk diameter measurements. Irrig Sci 20:115–125.

Heerema RJ, Weinbaum SA, Pernice F, DeJong TM (2008) Spur survival and return bloom in almond [*Prunus dulcis* (Mill.) D.A. Webb] varied with spur fruit load, specific leaf weight, and leaf area. J Hort Sci Biotech 83:274–281.

Heilmeier H, Wartinger A, Erhard M, Zimmermann R, Horn R, Schulze ED (2002) Soil drought increases leaf and whole-plant water use of *Prunus dulcis* grown in the Negev Desert. Oecologia 130:329–336.

Jifon JL, Syvertsen JP (2003) Moderate shade can increase net gas exchange and reduce photoinhibition in citrus leaves. Tree Physiol 23:119–127.

Jones HG (1992) Plants and microclimate: a quantitative approach to environmental plant physiology. Cambridge University Press, Cambridge, UK.

Le Roux X, Grand S, Dreyer E, Daudet FA (1999) Parameterization and testing of a biochemically based photosynthesis model for walnut (*Juglans regia*) trees and seedlings. Tree Physiol 19:481–492.

Massonnet C, Regnard JL, Lauri PE, Costes E, Sinoquet H (2008) Contributions of foliage distribution and leaf functions to light interception, transpiration and photosynthetic capacities in two apple cultivars at branch and tree scales. Tree Physiol 28:665–678.

Matos MC, Matos AA, Mantas A, Cordeiro V, Vieira da Silva JB (1998) Diurnal and seasonal changes in *Prunus amygdalus* gas exchanges. Photosynthetica 35:517–524.

Medhurst J, Parsby J, Linder S, Wallin G, Ceschia E, Slaney M (2006) A whole-tree chamber system for examining tree-level physiological responses of field-grown trees to environmental variation and climate change. Plant Cell Environ 29:1853–1869.

Muraoka H, Koizumi H (2005) Photosynthetic and structural characteristics of canopy and shrub trees in a cool-temperate deciduous broadleaved forest: implication to the ecosystem carbon gain. Agric For Meteorol 134:39–59.

Niinemets Ü, Kuhn U, Harley PC et al. (2011) Estimations of isoprenoid emission capacity from enclosure studies: measurements, data processing, quality and standardized measurement protocols. Biogeosciences 8:2209–2246.

Nortes PA, González-Real MM, Egea G, Baille A (2009) Seasonal effects of deficit irrigation on leaf photosynthetic traits of fruiting and non-fruiting shoots in almond trees. Tree Physiol 29:375–388.

Palva L, Markkanen T, Siivola E et al. (2001) Tree scale distributed multipoint measuring system of photosynthetically active radiation. Agric For Meteorol 106:71–80.

Pearcy RW, Yang W (1996) A three-dimensional crown architecture model for assessment of light capture and carbon gain by understory plants. Oecologia 108:1–12.

Pearcy RW, Muraoka H, Valladares F (2005) Crown architecture in sun and shade environments: assessing function and trade-offs with a three-dimensional simulation model. New Phytol 166: 791–800.

Pérez-Pena JE (2004) Whole-canopy photosynthesis and transpiration under regulated deficit irrigation in *vitis vinifera* L. cv. Cabernet Sauvignon. Doctoral thesis, Washington State University, Pullman, WA, USA, 234 p.

Planchais I, Sinoquet H (1998) Foliage determinants of light interception in sunny and shaded branches of *Fagus sylvatica* (L.). Agric Forest Meteorol 89:241–253.

Rijkers T, Pons TL, Bongers F (2000) The effect of tree height and light availability on photosynthetic leaf traits of four Neotropical species differing in shade tolerance. Funct Ecol 14:77–86.

Sinoquet H, Le Roux X (2000) Short term interactions between tree foliage and the aerial environment: an overview of modelling approaches available for tree structure–function models. Ann For Sci 57:477–496.

Sinoquet H, Le Roux X, Adam B, Ameglio T, Daudet FA (2001) RATP: a model for simulating the spatial distribution of radiation absorption, transpiration and photosynthesis within canopies: application to an isolated tree crown. Plant Cell Environ 24:395–406.

Synkova H, Semoradova S, Schnablova R, Müller K, Pospisilova J, Ryslava H, Malbeck J, Cerovska N (2006) Effects of biotic stress caused by potato virus Y on photosynthesis in ipt transgenic and control *Nicotiana tabacum* L. Plant Sci 171:607–616.

Valladares F, Dobarro I, Sanchez-Gomez D, Pearcy RW (2005) Photoinhibition and drought in Mediterranean woody saplings: scaling effects and interactions in sun and shade phenotypes. J Exp Bot 56:493–504.

Walcroft AS, Lescourret F, Génard M, Sinoquet H, Le Roux X, Donés N (2004) Does variability in shoot carbon assimilation within the tree crown explain variability in peach fruit growth? Tree Physiol 24:313–322.